Factors Controlling the Net Ecosystem Production of Cryoconite on Western Himalayan Glaciers

Monica Sharma Shamurailatpam[1], Jon Telling[2], Jemma L Wadham[3,4,5], AL. Ramanathan[1], Chris Yates[5], N Janardhana Raju[1]

[1] School of Environmental Sciences, Jawaharlal Nehru University, New Delhi, India

[2] School of Natural and Environmental Sciences, Newcastle University, Newcastle, UK

[3] Centre for Arctic Gas Hydrate, Environment and Climate, UiT the Arctic University of Norway, Tromsø, Norway

[4] Centre for ice, Cryosphere, Carbon and Climate, UiT the Arctic University of Norway, Tromsø, Norway

[5] School of Geographical Sciences, University of Bristol, Bristol, UK

Corresponding author email: monica.shamurai@gmail.com

Abstract:

In situ experiments were conducted to determine the Net Ecosystem Production (NEP) in cryoconite holes from the surface of two glaciers (Patsio glacier and Chhota Shigri glacier) in the Western Himalaya during the melt season from August to September 2019. The study aimed to gain an insight into the factors controlling microbial activity on glacier surfaces in this region. A wide range of parameters, including sediment thickness, TOC %, TN %, chlorophyll-*a* concentration, altitudinal position, and grain size of the cryoconite mineral particles were considered as potential controlling factors. From redundancy analysis, the rate of Respiration observed in cryoconite at Chhota Shigri glacier was predominantly explained by sediment thickness in cryoconite holes (37.1 % of the total variance, $p < 0.05$) with Photosynthesis largely explained by the chlorophyll-*a* content of the sediment (39.6 %, $p < 0.05$). NEP was explained primarily by the TOC content and sediment thickness in cryoconite holes (35.8 % and 22.1 % respectively, $p < 0.05$). The altitudinal position of the cryoconite is strongly correlated with biological activity, suggesting that the stability of cryoconite holes was an important factor driving primary productivity and respiration rate on the surface of Chhota Shigri glacier. We calculated that the number of melt seasons required to accumulate organic carbon in thin sediment layers (<0.3 cm), based on our measured NEP rates, ranged from 11 to 70 years, indicating that the organic carbon in cryoconite holes largely derives from allochthonous inputs, such as elsewhere on the glacier surface. Phototrophic biomass in the same thin sediment layer of cryoconite was estimated to take atleast 4 months to be produced *in situ* (with mean estimated time upto 1.7 ± 1.5 years). Organic matter accumulated inside the cryoconite holes both through allochthonous deposition

and via biological activity on the glacier surface in these areas may have the potential to export dissolved organic matter and associated nutrients to downstream ecosystems. Given the importance of Himalayan glaciers as a vital water source for millions of people downstream, this study highlights the need for further investigation in aspects of the quantification of *in situ* produced organic matter and its impact on supraglacial melting in the Himalaya.

Keywords: Net Ecosystem Production, Respiration, Western Himalaya, Cryoconite holes, Biological activity.

1. Introduction:

The Himalayan region has experienced a 40 % loss of its glacier area since the Little Ice Age maximum (1300 CE to 1600 CE), and glaciers melting has accelerated by 10 times in the past few decades (Lee et al. 2021). Several studies have reported the accelerating loss of ice across Himalayan glaciers due to a changing climate (Fujita and Nuimura 2011; Bolch et al. 2012; Azam et al. 2014a; Zhao et al. 2016; Mandal et al. 2016; Maurer et al. 2019; Garg et al. 2021). Future projections for high-altitude Asian glaciers indicate at least a 50 % loss of current ice mass and volume by mid-century as climate change intensifies (Zhao et al. 2014; Rounce et al. 2020). The loss of glacier area and volume across the Himalayan region is of particular concern, since it has both social and environmental implications, with a number of challenges associated with water supplies and future aggravated ecosystem and environmental degradation (Bakke et al. 2016; Pritchard 2017; Higgins et al. 2018; Bolch et al. 2019).

The supraglacial environment is the uppermost part on the glacier surface that interacts directly with the atmosphere and receives direct solar radiation and thus responds to external climate forces through accelerating surface melting. One of the potential factors which might accelerate the rapid decline of glacier ice areas and volume due to atmospheric warming and precipitation changes is a reduction of surface albedo due to the accumulation of organic and inorganic particles called “cryoconite” in the supraglacial environment (Takeuchi et al. 2000, 2001, 2010; Hodson et al. 2010b). Cryoconite is produced locally from the melt-out of glacial sediments, inputs of aeolian dust, alongside biological productivity and can be found disperse on snow and ice surfaces, thereby causing the darkening of glaciers (Takeuchi et al. 2001; Remias et al. 2005; Qian et al. 2015; Musilova et al. 2016; Stibal et al. 2017). Thin cryoconite layers on glacier surfaces has the potential to absorb solar radiation due to its low reflectivity, and can form cylindrical depressions on the glacier surface known as ‘cryoconite holes’ (Fountain et al. 2004; Telling et al. 2012). These serve as habitats for autotrophic microorganisms, including bacteria, algae (Anesio et al. 2009) and as well as other heterotrophic microbial communities in the wider glacial ecosystem (Zarsky et al. 2013; Nicholes et al. 2019; Rozwalak et al. 2022). Due to the presence of liquid water,

light, and nutrients (Stibal et al. 2008) during the ablation period, microorganisms in cryoconite holes can display significant rates of metabolism (Foreman et al. 2007; Edwards et al. 2011) with high primary production and respiration rates that are comparable to those of eutrophic ecosystems in warmer regions (Anesio et al. 2009). Cryoconite holes also provide a protective aquatic environment on glacier surfaces for microorganisms from extreme UV radiation, temperature fluctuations and changes in environmental conditions by forming ice lids over the granules (Hodson et al. 2010b; Langford et al. 2014; Bagshaw et al. 2016). However, depending on the time of the year, surface temperature variability and meltwater connectivity, the structure and microbial abundance within the cryoconite holes may vary both temporally and spatially (Lutz et al. 2017; Pittino et al. 2018), which may affect the microbial activity on the glacier surface. Microorganisms trapped in cryoconite holes often display high net biological productivity, resulting in organic matter accumulation in supraglacial ecosystems (Hodson et al. 2007; Telling et al. 2012). This produces dark-coloured material which can further reduce the albedo of the glacial surface, a process known as the 'bio-albedo effect' (Takeuchi et al. 2001; Cook et al. 2017). However, studies investigating these biological-melt feedbacks have largely been conducted on Arctic and Antarctic glaciers (Säwström et al. 2002; Hodson et al. 2005; Stibal et al. 2008; Uetake et al. 2010; MacDonell and Fitzsimons 2012; Zarsky et al. 2013; Bagshaw, et al. 2013; Lutz et al. 2017; Holland et al. 2019; Leidman et al. 2021).

Previous studies in the Himalaya have demonstrated the presence of diverse microbial communities on glacier surfaces (Sanyal et al. 2018), and inferred the biological production of organic matter via biomarkers and geochemical tracers (Nizam et al. 2020). Organic matter formed on the glacier surface can be largely autochthonous produced through *in situ* photosynthesis on the glacier surface (Anesio et al. 2009; Telling et al. 2010, 2012). A similar conclusion was drawn by Nizam et al. (2020) in their study on glacier surfaces of the Western Himalaya, however, their study lacked experimental data to confirm the operation of biological processes, or their potential direct impact on organic matter accumulation, and potential surface darkening. Here we conducted a suite of experiments to directly determine for the first time the potential biological productivity of microorganisms in cryoconite holes of two glaciers, Patsio and Chhota Shigri glaciers in the Western Indian Himalaya, with an emphasis on identifying the factors controlling the Net Ecosystem Production (NEP) in surface microbial ecosystems.

2. Methods:

2.1. Study Area

Fieldwork was conducted at Chhota Shigri Glacier (32.23˚ N, 77.51˚ E) and Patsio Glacier (32.7˚ N, 77.3˚ E), Lahaul-Spiti Valley, Himachal Pradesh, in August – September 2019. Chhota Shigri Glacier and Patsio glacier are both located in the Western Himalaya, situated 55 km apart. Chhota Shigri glacier is situated at an altitudinal range of 4050 – 6263 m a.s.l. and covers a total area of 15.5 km^2 while Patsio lies between 4875 – 5718 m a.s.l. with a total area of 2.25 km^2. Both Chhota Shigri and Patsio Glacier are largely debris-free glaciers with 11 % debris-covered for Chhota Shigri (Garg et al. 2017), mostly in the lower elevation < 4500 m a.s.l., while Patsio Glacier is approximately 12 % debris-covered (Angchuk et al. 2021). The climatologies of both glaciers are dominated by westerly winds during winter and less intensely by the Indian Summer Monsoon (ISM) during summer. The mean annual precipitation at Chhota Shigri and Patsio glaciers is 976 mm (2012 – 2013) (Azam et al. 2014b) and 585 mm (2010 – 2017) (Angchuk et al. 2021) respectively. The slopes at the Chhota Shigri and Patsio glaciers are 10˚ - 45˚ (Mandal et al. 2020) and 10˚ - 50˚ (Kumari et al. 2021) respectively (Fig 1 c-d). The mean air temperature during summer (June – September) in Chhota Shigri ranges from 1.9 to 4.3˚C (2009 to 2019) (Mandal et al. 2020) and in Patsio glacier from 1.7 to 2.3˚C (2015 to 2017) (Angchuk 2020). The summer ablation season last from mid-June to the end of September in this region (Azam et al. 2014b) with July and August reportedly the warmest months during the summer period in Chhota Shigri (Mandal et al. 2020) and July in Patsio (Angchuk 2020). Incubation experiments were carried out in the ablation zones of both glaciers (see Table 2 and Fig. 1).

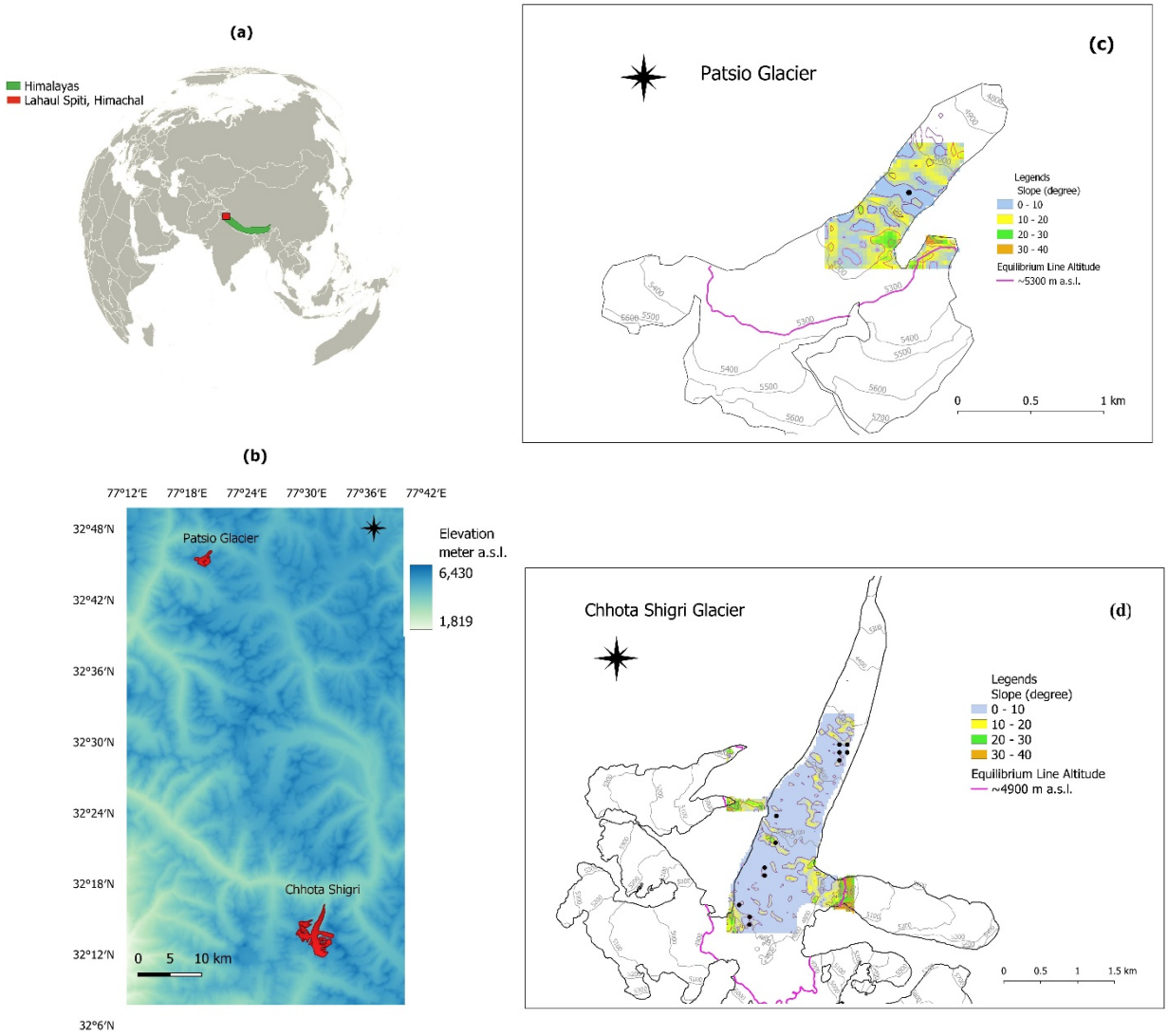

Fig. 1 Map showing the location of (a) The Himalayan regions, and of Lahaul Spiti, Himachal Pradesh, India, (b) Patsio Glacier and the Chhota Shigri Glacier in Lahaul Spiti Valley, (c) Chhota Shigri Glacier (d) and Patsio Glacier (Sampling points for experiments in (c) and (d) are shown at different elevations alongside the glacier surface) (Map coordinates are given in the Lat/ Long using the World Geodetic System 1984 (WGS84) reference system, maps (slopes and elevations) were generated using QGIS 3.22.)

2.2. **Measurements of *in situ* Net Ecosystem Production and Respiration**

Field experiments were performed in August - September 2019 to determine rates of Respiration and Net Ecosystem Production in cryoconite holes on both the surfaces of Chhota Shigri and Patsio Glaciers. A total of 16 sites (cryoconite holes) were chosen on both glaciers for *in situ* experiments (12 cryoconite sites in Chhota Shigri and 4 cryoconite sites in Patsio were intended; however, two of the experiments were lost due to breakages).

The experiments were performed over a large altitudinal gradient in Chhota Shigri glacier's ablation zone (between ~ 4500-4800 m a.s.l.) and at 5050 m a.s.l. in Patsio glacier. Cleaned and autoclaved BOD bottles of 30 mL were used for the experiments. One BOD bottle was covered with aluminium foil to represent (dark only) Respiration, while another was left uncovered to represent NEP (light only). Both bottles were filled with approximately the same amount of sediment, with a thickness range of 0.2 – 0.8 cm measured using a measuring tape to represent typical *in situ* thicknesses at the sampling sites. Similarly, one dark and one light blank bottle filled with stream water containing no sediment were taken to observe the influence of water only during Respiration and NEP respectively. Using a portable DO meter (Hach HQ40d DO meter), the initial concentration of dissolved oxygen (mg L^{-1}) was measured in all bottles. The BOD bottles were then left on the glacier surface completely submersed inside the cryoconite holes water. Where the holes were broken, the bottles were left exposed on the glacier surface in bare cryoconite. Final dissolved oxygen concentrations were measured after 24 ± 2 hours. Using the light and dark incubation, the rates of NEP and Respiration respectively were directly estimated (Hodson et al. 2010a; Telling et al. 2012) in units of µg C $L^{-1}day^{-1}$. Measurements were corrected with the dry sediment weight of cryoconite and converted to µg C $g^{-1}day^{-1}$. The primary production or Photosynthesis rate (autotrophy) is calculated as the sum of NEP and Respiration (Hodson et al. 2010a) :

$$P = NEP + R \quad (1)$$

Where P = rate of Photosynthesis, R = rate of Respiration in µg C $L^{-1}day^{-1}$ (or µg C $g^{-1}day^{-1}$).

2.3. Chlorophyll-*a* content in the cryoconite sediments

Cryoconite samples were stored soon after collection in a portable field freezer at sub-zero (-10 to -20˚C) temperatures in the dark and brought to the LOWTEX laboratory, University of Bristol. They were stored frozen until analysis which was conducted within three to four months. All extraction procedures for chlorophyll-*a* were conducted in low light conditions to avoid degradation. Frozen cryoconite sediments were weighed in pre-weighed 15 mL Falcon tubes covered with aluminium foil. The initial weight of the sediment was noted to determine the moisture content, and in order to later normalise the pigment concentration to the dry weight of sediment. Chlorophyll extraction was performed using 90 % acetone which was added to the pre-weighed Falcon tubes to completely cover the sediment, and the solution was mixed for two minutes on a vortex shaker. The Falcon tubes were then sonicated in an ice-chilled sonicator bath (>10˚C) for 20 minutes and kept at -4˚C for 24 hours. The tubes were vortexed again for 5 minutes, followed by centrifugation at 1500 rpm. The supernatants were then filtered through a 0.2 µm Whatman Puradisc Nylon membrane syringe filters and subsequently analysed for the

chlorophyll-*a* concentration using a UV-vis spectrophotometer. To report chlorophyll-*a*, as corrected for pheophytin content, absorption both before and after acidification of the extracts was measured at wavelength 665 nm and another at 750 nm for turbidity correction. Estimation of the chlorophyll-*a* concentration was conducted following Lorenzen (1967) and normalised to the dry weight of sediment. The limit of detection of the chlorophyll-*a* calculated using six blank acetone samples was 0.03 ± 0.17 µg L^{-1}.

2.4. Grain Size Distribution of the cryoconite minerals

Dry sediment samples were combusted in a furnace for 3 hours at 950˚ C to remove organic carbon and carbonated matter. Particles larger than 2 mm were removed with a sieve after loosely separating the particles with a pestle and mortar. The sample grain sizes were then measured using a Malvern MS3000 Mastersizer. Analyses were conducted in triplicate for each sample and a blank sample (water only) was run in between sample analyses. The mean value of the triplicate sample was reported for the grain size distribution.

2.5. Elemental Composition of the cryoconite of Chhota Shigri

The carbon, nitrogen and sulfur content of cryoconite from all sites were analyzed using a CHNS Vario PYRO cube Elemental Analyzer. The sediment was dried at 108 °C overnight, finely ground with a pestle and mortar, and passed through a 150 mesh sieve. Approximately 10 mg of the untreated samples were carefully sealed in aluminium capsules to measure the Total Carbon (TC) content. The Total Organic Carbon (TOC) content of the cryoconite constituted averaged 98 % of the TC in a sub-set of cryoconite sediment samples collected during August 2019 (Table 1). Due to the negligible Total Inorganic Carbon (TIC) content, TC for the present study were reported as TOC. The instrumental limit of detection was 0.001 % or 10 ppm.

Table 1 Total Carbon (TC), Total Organic Carbon (TOC) and Total Inorganic Carbon (TIC) in dry weight mass percentage from a sub-set of cryoconite sediment samples of Chhota Shigri glacier, collected during August 2019.

Cryoconite	TC (%)	TOC (%)	TIC (%)
CRY II	0.54	0.64	0.00
CRY V	1.22	1.22	0.00
CRY VI	0.48	0.31	0.17
CRY VII	1.76	1.91	0.00
CRY VIII	1.38	1.07	0.31

O	1.38	1.50	0.00
CRY V (d)	1.11	1.03	0.08
CRY VII (d)	0.12	0.12	0.00
CRY XI (d)	2.31	2.25	0.06
Mean	1.14	1.12	0.07

2.6. Statistical analysis

Multivariate statistical analyses were performed using the software package R (version 4.0.0). Redundancy discriminant analysis (RDA) was used to determine the impact of independent variables (explanatory variables) on dependent variables (response variables) in the data set. This statistical methodology extracts and summarizes the variation of the response variable that can be explained by a series of explanatory variables (Borcard et al. 2011).

3. Results:

3.1. Physical and Chemical Properties of Cryoconite Holes

Cryoconite hole diameter, depth, water depth and sediment thickness were measured at the experimental sites at Chhota Shigri and Patsio glaciers (Table 1). The sampling sites for *in situ* cryoconite in Chhota Shigri glacier were grouped according to elevation as "lower", "middle" and 'upper' sites, which corresponded to glacier slopes of 13˚ - 23˚, 10˚ - 19˚ and 10˚ - 12˚ respectively. Cryoconite holes observed in the lower site in Chhota Shigri (4562 m a.s.l.) were observed to be mostly broken, and scattered due to the connection of multiple channels and sediment exposed on the ice surface (Fig 2 A1-A2). Cryoconite holes at middle elevation sites of Chhota Shigri (4678 – 4747 m a.s.l.) were larger in size and possibly formed due to fusion of several cryoconite holes to form a larger hole. Multiple surface streams were also observed alongside at this site. At the upper sites in the Chhota Shigri and Patsio Glaciers, the cryoconite holes were circular shaped and smaller in size compared to the middle sites and were relatively stable and hydrologically isolated.

Table 2 Table showing the observed diameter, depth, water depth and sediment thickness of some of the cryoconite holes at different altitude in the Chhota Shigri and at the experimental site in Patsio Glacier.

Sites	Altitude (m a.s.l.)	Diameter (cm)	Depth (cm)	Water depth (cm)	Sediment Thickness (mm)
Lower	4562	*	n.d	n.d	n.d
Middle	4747	35	13	6	>0.5

	4678	30	15	8	0.2
Upper	4760	12	14	4	0.2
	4789	17	14	5.5	>0.2
Patsio Glacier	5050	11	11	9.5	>0.2
	5050	10	19	16	>0.2

* - scattered cryoconite holes
n.d - not applicable

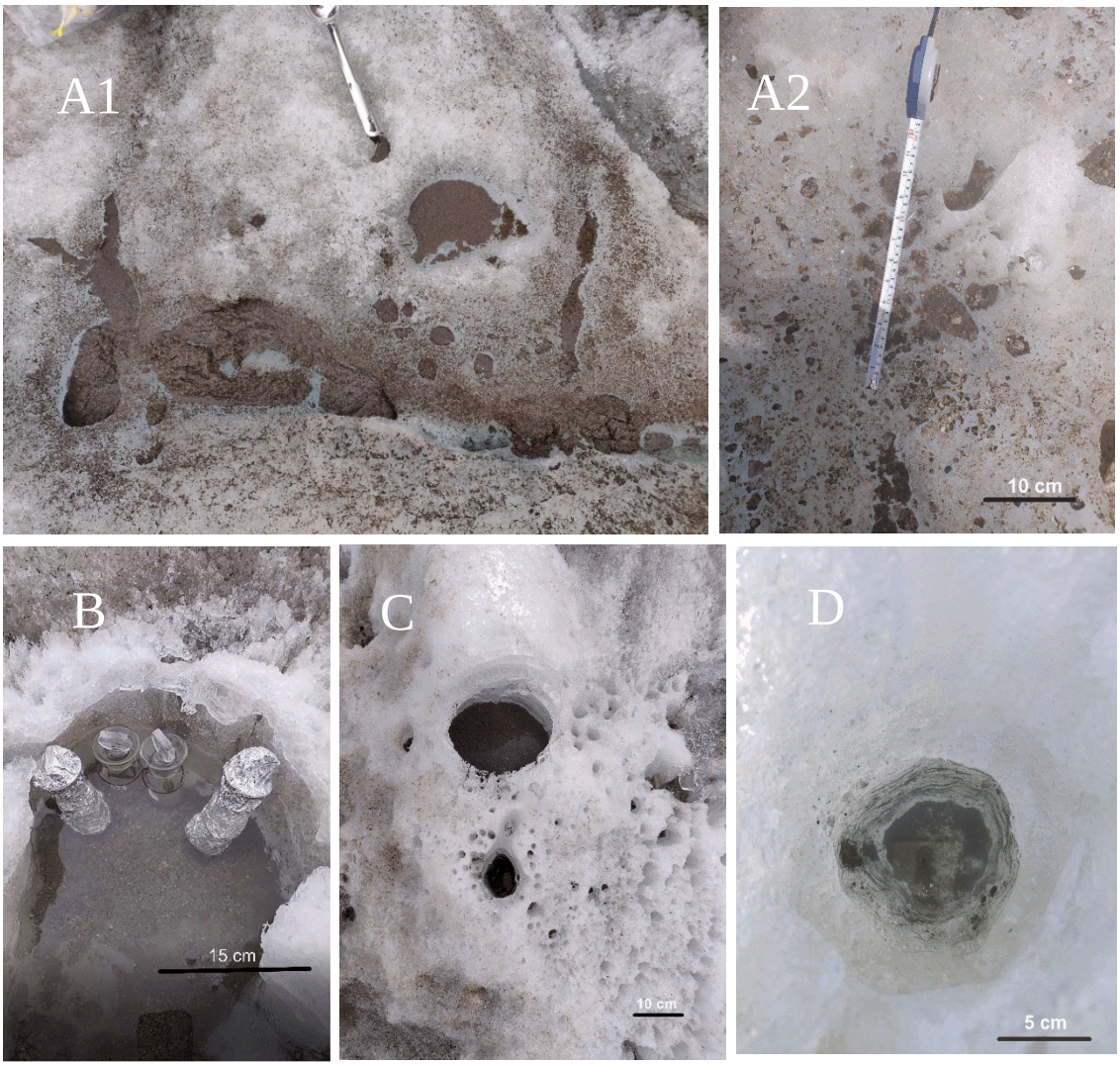

Figure (A1-A2) cryoconite in lower ablation, (B) cryoconite hole in middle ablation sites (C) cryoconite hole at upper sites at Chhota Shigri Glacier and (D) cryoconite hole at Patsio Glacier

A summary of the parameters measured is given in Table 3. A scatter matrix diagram comprising a scatter plot, distribution diagram, boxplot, and Pearson correlation of all the parameters is given in Fig. 3.

Table 3 Mean and standard deviation (±) of physical and chemical properties of the cryoconite sediment on the surface of the Chhota Shigri (CS) and Patsio glaciers

Cryoconite position on the glacier surface	Elevation (m)	TN %	TOC %	Chlorophyll-*a* (μg g^{-1})	Grain size (μm)	S:C	C:N
Patsio (n = 2)	5050	0.21 ± 0.01	2.38 ± 0.02	12.6 ± 2.30	45.65 ± 1.20	0.08	11.35
CS upper sites (n =3)	4789 - 4760	0.20 ± 0.06	1.81 ± 0.59	8.41 ± 1.50	39.64 ± 0.69	0.01	9.09
CS middle sites (n =4)	4678 - 4747	0.08 ± 0.05	0.68 ± 0.46	5.30 ± 2.00	63.30 ± 25.40	0.03	8.99
CS lower sites (n =5)	4562	0.06 ± 0.03	0.52 ± 0.29	3.60 ± 1.25	62.9 ± 16.9	0.07	8.92

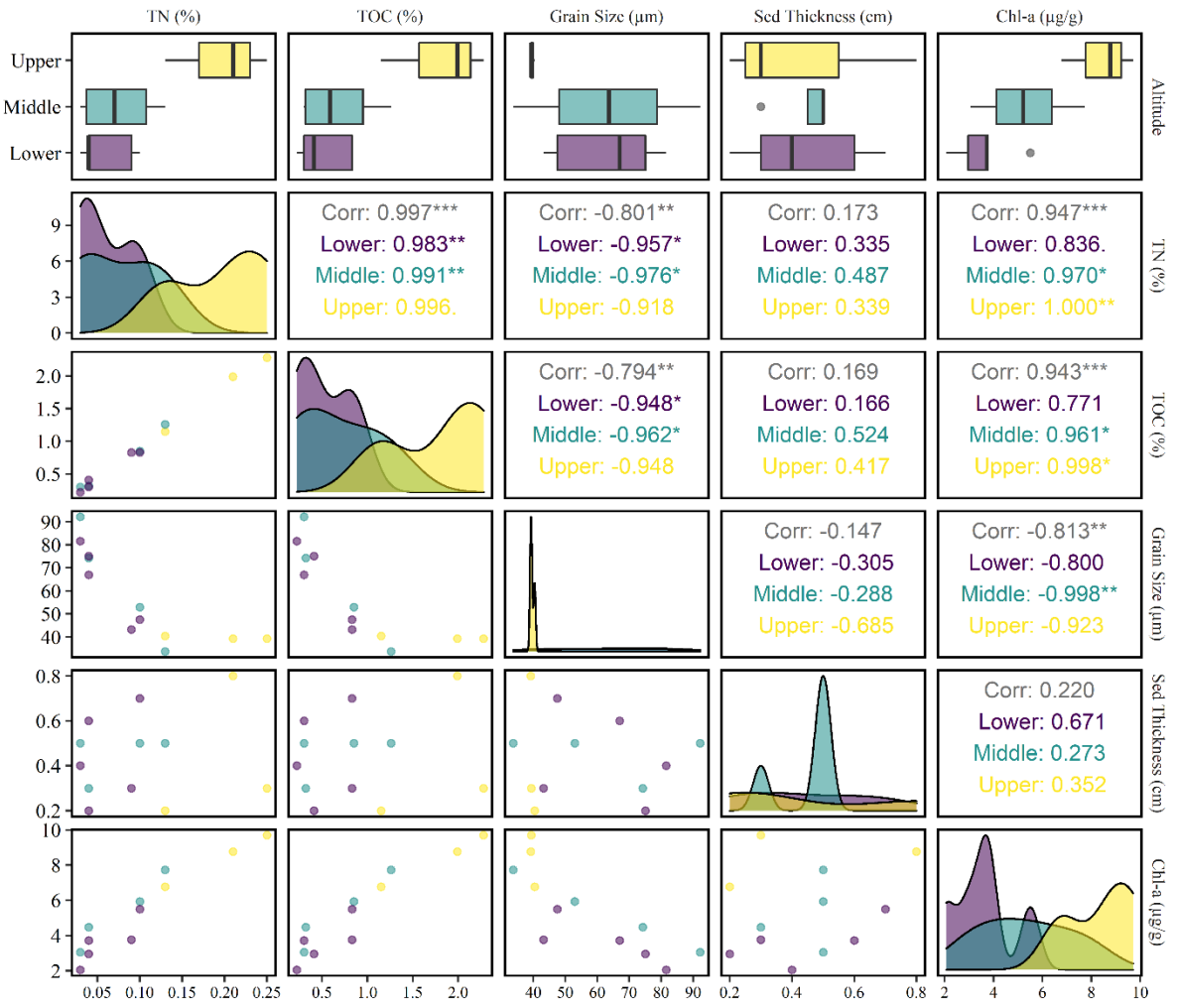

Fig. 3 Scatter matrix diagram of all parameters (TN, TOC, grain size, sediment thickness and Chlorophyll-*a*) measured in cryoconite holes on the glacier surface at the lower, middle and upper elevations of Chhota Shigri Glacier

The TOC and TN content of cryoconite showed an overall significant positive correlation with chlorophyll-*a* (df = 10, r =0.94 and 0.94 respectively, p<0.01 (Fig.3), R^2 = 0.88 and 0.89 respectively, p <0.001 (Additional File Fig A2)). The TOC, TN and chlorophyll-*a* content of the cryoconite increased from the lower and middle to the upper sites in the Chhota Shigri Glacier (Fig.3), with mean values increasing from 0.52 and 0.68 to 1.81 % for TOC, 0.06 and 0.08 to 0.20 % for TN and 3.62 and 5.3 to 8.4 µg g^{-1} for chlorophyll-*a* content from lower and middle to upper sites (Table 3). In Patsio glacier, the observed mean TOC (2.38 %), TN (0.21 %) and chlorophyll-*a* content (12.6 µg g^{-1}) were close to that of the upper sites at Chhota Shigri Glacier. In addition, the mean grain size of the cryoconite minerals in the upper region at Chhota Shigri and at Patsio glaciers (39.60 µm and 45.65 µm

respectively) was smaller than that of the lower (62.88 µm) and middle (63.30 µm) sites at the Chhota Shigri glacier. The TOC content of cryoconite lacked a statistically significant association with sediment thickness ($r = 0.16$, $df = 10$, $p > 0.05$); but did show a significant negative correlation with the mean grain size of the cryoconite mineral particulate (TOC, $R^2 = 0.59$, slope =-23, $df = 10$, $p = 0.002$ (Additional File)). Similarly, TN and chlorophyll-a were significantly negatively associated with the mean grain size of cryoconite mineral particulate matter (TN and chlorophyll-*a*, $R^2 = 0.61$, $p = 0.0017$ and 0.63, $p = 0.0013$ respectively, $df = 10$ (Additional File)). The mean C:N ratios in the cryoconite were 8.9 – 11.3, which is similar to well-decomposed organic matter as observed in glaciers in the Himalayas and Arctic (Takeuchi 2002). The mean S:C ratios were 0.01 – 0.07, largely consistent with ratios reported for microbial cells (range 0.016 to 0.084, Fagerbakke et al., 1996).

3.2. Measurement of Microbial Productivity

The rate of Photosynthesis calculated from the 24 ± 2 hours incubations in the BOD bottles containing cryoconite at the lower, middle and upper experimental sites at Chhota Shigri and Patsio glacier ranged from 180 to 375 µg $C\,L^{-1}\,day^{-1}$, 210 to 491 µg $C\,L^{-1}day^{-1}$, 588 to 937 µg $C\,L^{-1}day^{-1}$ and 1162.5 to 1200 µg $C\,L^{-1}day^{-1}$ respectively, with mean values given in Table 4. The rate of Respiration ranged from 225 to 405 µg $C\,L^{-1}day^{-1}$ (lower sites), 378 to 656 µg $C\,L^{-1}day^{-1}$ (middle sites) , 401 to 825 µg $C\,L^{-1}day^{-1}$ (upper sites) at Chhota Shigri and 521 to 577 µg $C\,L^{-1}day^{-1}$ at Patsio glacier. The rates of NEP were -217 to 123 µg $C\,L^{-1}day^{-1}$ (lower sites), -206 to -22 µg $C\,L^{-1}day^{-1}$ (middle sites) and 112 to 236 µg $C\,L^{-1}day^{-1}$ (upper sites) and 585 to 678 µg $C\,L^{-1}day^{-1}$ (Patsio). On average, rates of Photosynthesis and Respiration in the water only incubations were 3 to 4 times lower than in those in the bottles containing cryoconite (Table 4). In general, sediment layers of thickness of approximately <0.3 cm were generally dominated by net autotrophy (mean of 251 µg $C\,L^{-1}day^{-1}$) while cryoconite with thicknesses of ≥0.5 cm were dominated by net heterotrophy (mean of -163 µg $C\,L^{-1}day^{-1}$) (Fig. 4) at both glaciers. Cryoconite at the upper sites and Patsio glacier displayed higher rates of Photosynthesis and Respiration compared to the lower and middle sites at Chhota Shigri (Table 4).

Table 4 Table showing the mean and ± 95% confidence interval of *in situ* measurement of Respiration (R), NEP, and Photosynthesis (P) (all units in µg $C\,L^{-1}day^{-1}$) in cryoconite and blank water sample constituting stream water only from the Chhota Shigri (CS) and Patsio glaciers

Cryoconite position	$P_{cryoconite}$	$R_{cryoconite}$	$NEP_{cryoconite}$	$P_{water\ only}$	$R_{water\ only}$	$NEP_{water\ only}$
Patsio (n = 2)	1181.25 ± 26.52	549.38 ± 39.77	631.88 ± 66.29	170.63 ± 66.29	129.38 ± 135.23	41.25 ± 68.94
CS upper (n = 3)	728.75 ± 184.26	550.00 ± 238.42	178.75 ± 62.34	145.00 ±50.91	112.50 ± 52.10	32.50 ± 5.73
CS middle (n = 4	361.88 ± 131.50	512.81 ± 113.51	-150.94 ± 87.43	142.50 ± 80.72	96.56 ± 73.44	45.94 ± 94.94
CS lower (n = 5)	275.25 ± 89.70	307.50 ± 71.59	-32.25 ± 147.25	143.25 ± 119.89	124.50 ± 62.49	18.75 ± 65.65

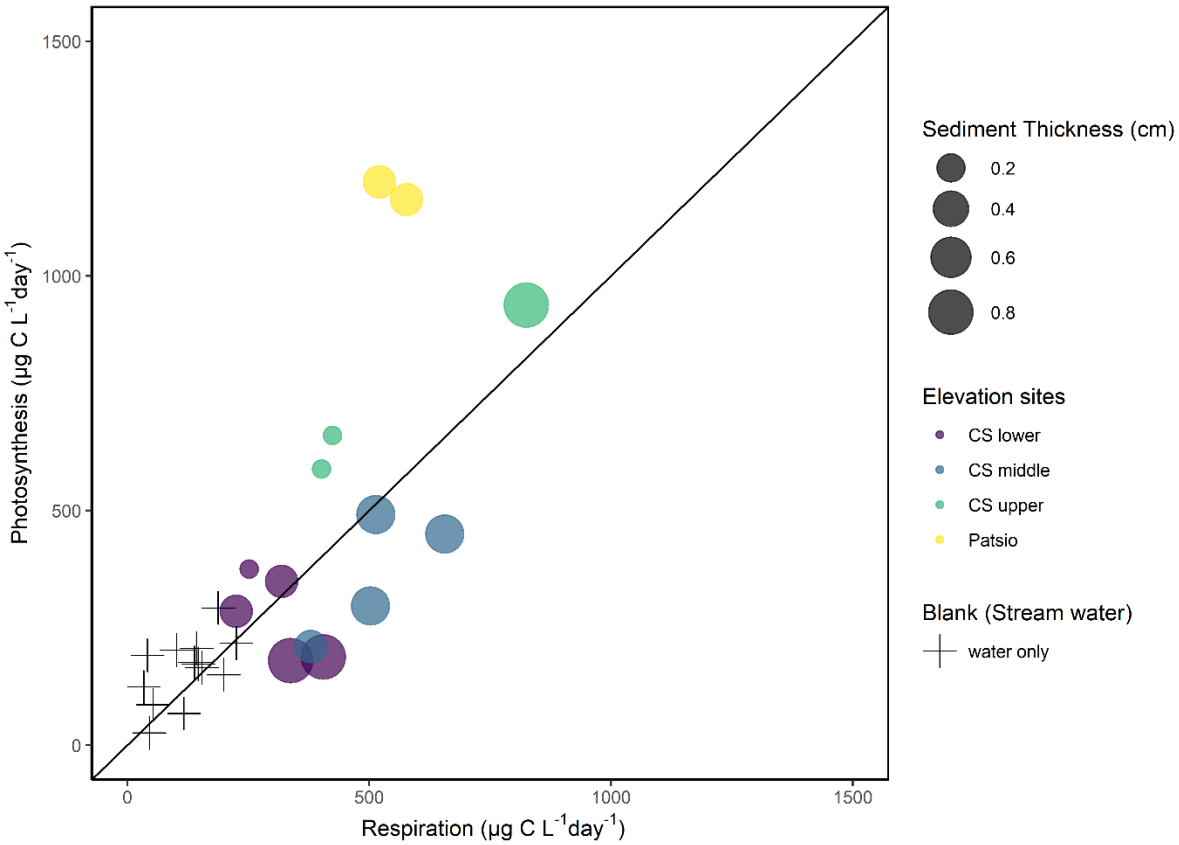

Fig. 4 Association between Respiration and Photosynthesis in cryoconite and water only (stream water without cryoconite) at different elevation sites at Chhota Shigri (CS) and Patsio glaciers

3.3. Multivariate Statistical Analysis

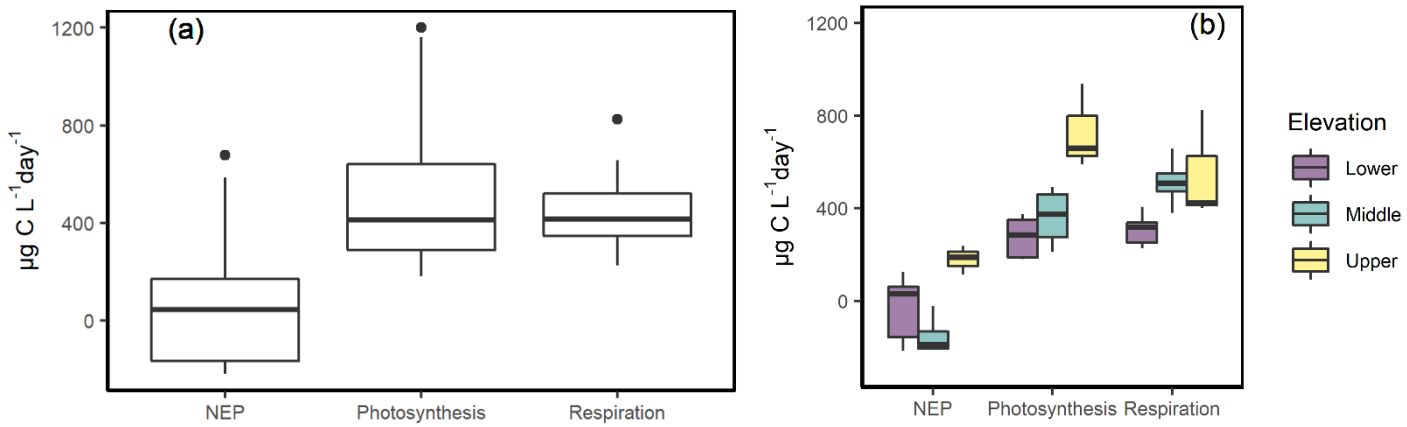

Fig. 5 (a) Box plots of NEP, Photosynthesis and Respiration rates observed at Chhota Shigri and Patsio glacier, (b) Box plots of NEP, Photosynthesis and Respiration distribution (in the lower, middle and upper regions of Chhota Shigri glacier)

To infer the controls upon microbial activity in the cryoconite holes, multivariate statistical analyses were performed. NEP, Photosynthesis and Respiration were taken as dependent variables with sediment thickness, TOC %, TN %, Chlorophyll-*a*, elevation, and grain size as independent variables. Boxplots of Respiration, NEP and Photosynthesis are presented in Fig. 5. Detrended correspondence analysis (DCA) was performed in order to determine the appropriate model to describe the association of the variables. The length of the axis ordination was 0.85 SD, therefore, redundancy analysis was determined as a suitable model to define the relationship between the variables. Before performing the ordination, all variables were standardized prior to the RDA. Since TN showed high collinearity with other parameters, it was therefore excluded from the model calculation to prevent overfitting of the model. The result of the RDA plot is given in Figure 7 with manual forward selection using NEP, Photosynthesis and Respiration as dependent variables. Based on the multivariate analysis, sediment thickness, altitude, chlorophyll-*a* and TOC were identified as the highly significant explanatory variables ($p<0.05$) for the overall productivity and microbial activity (NEP, Photosynthesis and Respiration) in cryoconite holes (Table 6). The most significant variables explaining the NEP was TOC, which explained 35.9 % of the total variance, (df = 1, F value = 9.7, p = 0.021), alongside sediment thickness which explained 22.1 % (df = 1, F value = 6.0, p = 0.04) of the total variance (74.2 %) in NEP. Out of the 82.3 % of the total variance in Photosynthesis, chlorophyll-*a* content accounted for 39.6 % (df = 1, F value = 15.7, p = 0.009), TOC accounting 24.6 % (df = 1,

F = 9.7, p = 0.23) and elevation accounted for 16.3 % (df = 1, F value = 6.5, p = 0.041) of the total variance. The model explained 95.1 % of the total variance in Respiration and identified three significant explanatory variables - sediment thickness accounting for 37.1 % (df = 1, F value = 53.72, p = 0.001), elevation accounting 33.1 % (df =2, F value = 47.9, p = 0.001) and chlorophyll-*a* accounting for 24.8 % (df = 1, F value = 36.0 p = 0.002).

4. Discussion

4.1. Factors controlling the microbial activity on the Himalayan glacial surface

The results of our study are consistent with previous work in other glaciated regions which has demonstrated that altitude, sediment grain size, cryoconite hole stability and other physical characteristics of the cryoconite on the glacier surfaces are important influencers of biological productivity in cryoconite holes (Langford et al. 2014; Chandler et al. 2015). In the upper sites at Chhota Shigri and Patsio glaciers, the cryoconite holes were hydrologically isolated, therefore the limited water movement and relative stability of the cryoconite in these sites may favour microbial growth (Langford et al. 2014). This was supported by the observed higher concentration of TOC, TN and chlorophyll-*a* content in these sites compare to lower sites where cryoconite holes were generally exposed and washed out due to greater hydrological connectivity. Also significant association of grain size of the cryoconite with TOC (R^2 = 0.59, df = 10, p = 0.002), TN (R^2 = 0.61, df = 10, p = 0.0017) and chlorophyll-*a* (R^2 = 0.63, df = 10, p = 0.0013) (Additional Files Fig. 3) was observed in our study. Fine cryoconite mineral particles dominated in the upper sites in Chhota Shigri and Patsio and the concentrations of TOC, TN and chlorophyll were subsequently higher. In contrast, at the lower region, the cryoconite grain size were coarser with a lower TOC, TN and chlorophyll content (Table 3). This observation corresponds with studies on Svalbard glaciers, where Kastovská et al. (2005) and Stibal et al. (2006) observed a high abundance of autotrophs and heterotrophs associated with cryoconite with a high proportion of fine sediments and with greater water retention time. The observed high organic content of finer cryoconite might reflect the greater nutrient availability for microbial activity than that of the coarser cryoconite at the lower site. Chlorophyll–*a* and TOC contents also increased with elevation, showing higher NEP values in the upper region (Fig. 5). The abundance of phototrophs and their potential productivity on glacier surfaces are often influenced by altitudinal gradients in mountain glaciers (Takeuchi et al. 2006; Takeuchi 2013), including the Himalaya (Yoshimura et al. 1997) where a general decrease in algal biomass is observed with altitude. These latter observations, however, were made on snow algal communities. Conversely, cryoconite holes present on the glacier's surface may provide a protective environment for these phototrophs to survive in the extreme conditions, depending on the local ice topography, shading,

availability of irradiance (Cook et al. 2018). This may explain why higher biomass and productivity were sustained on the Chhota Shigri at higher elevations, as discussed in detailed below.

An important factor contributing to the enhanced organic matter accumulation in the upper regions of our experimental sites is likely the relatively low hydrological connectivity and gentle glacier surface slopes which reduce disruption of the cryoconite holes compared with those located in the middle and lower glacier regions studied here. Greater hydrological stability may lead to the formation of stable aggregates (Samui et al. 2018) which support higher rates of biological activity, thereby enhancing the accumulation of autochthonous organic matter (Bagshaw, et al. 2013). From the statistical analysis, elevation (also related to the stability of cryoconite holes in the present study; Section 3.1) accounted for 16.3 % while TOC accounted for 24.6 % of the total variance in the Photosynthesis (Table 6). This observation suggests that the position of the cryoconite holes on the glacier surfaces has an influence on the primary productivity of cryoconite holes, and the consequent accumulation of organic matter. This is in alignment with a study by Stibal et al.(2012b), where enhanced microbial activity upslope on a glacier in Greenland resulted in increased organic matter accumulation because of less disturbance by flowing water on gentler ice surface slopes.

Another potential factor controlling the abundance of biomass production is the rate of Photosynthesis, which depends in part on the availability of photosynthetically active radiation (PAR) (Säwström et al. 2002; Cook et al. 2010). Although PAR was not measured in this study, the higher rate of Photosynthesis observed in the upper region in our experiments might be consistent with higher light availability for the autotrophs at a higher elevation compared to the lower elevations due to lower topographical shading. Multivariate statistical analysis also supported chlorophyll-*a* as being the most significant factor controlling the ecosystem production accounting for 39.6 % (df = 1, F value =15.7, p = 0.009) of the total variance in Photosynthesis (Table 6). The higher chlorophyll-*a* contents at the upper study sites are consistent with higher rates of Photosynthesis in these regions. The lack of a significant relationship between Photosynthesis and sediment thickness may also reflect light limitation in deeper layers of sediment (Telling et al. 2012).

The NEP rate of thin cryoconite sediment layers <0.3 cm were also observed to be consistent with net autotrophic conditions, while at sediment thicknesses of ≥ 0.5 cm, cryoconite generally exhibited net heterotrophy, due to greater rates of Respiration (Fig. 4). This effect was pronounced at lower and middle glacier sites compared to the cryoconite in the upper region. RDA analysis also showed that TOC and sediment thicknesses of the cryoconite

layer exert a significant control on NEP, accounting 35.8 % (df = 1, F value = 9.7, p = 0.021) and 22.1 % (df = 1, F value = 6.0, p = 0.04) respectively of the total NEP variation. It is also possible that the existence of various cryophilic invertebrates, such as copepods, tardigrades and rotifers reported in the Himalayan cryoconite holes (Kohshima et al. 2002; Zawierucha et al. 2021) may also contribute to the respiration although their contribution is not quantified here. The development of potential anaerobic microbial niche in thick cryoconite layers (~4 – 6 mm thickness) may also occur (Poniecka et al. 2018; Buda et al. 2021). From the RDA analysis, we found that sediment thickness explained 37.1 % of the total variance in Respiration (df = 1, F value = 53.7, p = 0.001), and chlorophyll content explained 24.8 % of the variance (df = 1, F value = 36.0, p = 0.002) (Table 6). We note these observations were drawn from a small sample size, and therefore, need to be further tested with different sediment thicknesses along the altitudinal gradients with a larger sample size. However, a similar association between thin sediment layers, fine grain size and enhanced NEP and organic matter in cryoconite holes were also observed in the upper ablation area of Greenland Ice Sheet (Cook et al. 2010; Stibal et al. 2010), as well as in Svalbard glaciers (Telling et al. 2012) and suggests that thicker sediment layers may directly influence heterotrophic activity in Himalayan cryoconite. We note as well that cryoconite net ecosystem production is also likely be altered by seasonality. For example, a study on an Alpine glacier demonstrated that cryoconite holes are generally dominated by heterotrophs later in the season, while in the early melt period autotrophs like cyanobacteria dominated (Pittino et al. 2018). NEP on Chhota Shigri was lowest at the middle parts of the ablation zones with net heterotrophy predominating at the lower sites, which were accompanied by decreased chlorophyll-*a* concentration, organic matter, and coarser cryoconite particles. The decrease in chlorophyll-*a* concentration and organic matter down-glacier can be attributed to the formation of new channels which increased meltwater flushing on steeper slopes during the melt season (Takeuchi 2013) resulting in the break up of cryoconite holes. This rapid hydrological flushing of meltwater channels can result in a trend towards a net heterotrophic conditions (Hodson et al. 2007; Telling et al. 2012). We compare our measured rates of NEP with those measured using similar methods in polar glaciers and ice sheets in Table 5. These show that our measured NEP rate fall within the range of those observed in the polar glaciers and ice sheets, and the measured net Respiration and Photosynthesis rates in the present study are more similar to those measured from the Antarctic Ice Sheet. The low net Respiration and Photosynthesis in the present Himalayan cryoconite holes, compared to that of Arctic glaciers, could reflect their shorter lifetime on Himalayan glacier surfaces (Takeuchi et al. 2000) which is explained in the following section.

366 **Table 5** Comparison of rates of Net Ecosystem Production (NEP), Photosynthesis (P) and Respiration (R) with

367 those of previous measurements of cryoconite in Polar Regions using similar method as the present study

Location		NEP	P	R	Unit	Source
Chhota Shigri, Lahaul Spiti, Western Himalaya (Lower)	Range	-1.63 – 2.86	1.41 – 8.67	2.73 – 5.81	µg C $g^{-1}day^{-1}$	Present study
	Mean ± SD	0.23 ± 1.81	3.83 ± 2.97	3.60 ± 1.26		
Chhota Shigri, Lahaul Spiti, Western Himalaya (Middle)	Range	-2.53 – -0.97	1.81 – 3.85	3.08 – 5.68	µg C $g^{-1}day^{-1}$	Present study
	Mean ± SD	-1.38 ± 0.97	3.05 ± 0.87	4.43 ± 1.13		
Chhota Shigri, Lahaul Spiti, Western Himalaya (Upper)	Range	0.68 – 3.52	5.63 – 11.04	4.54 – 7.52	µg C $g^{-1}day^{-1}$	Present study
	Mean ± SD	2.24 ± 1.44	7.91 ± 2.80	5.67 ± 1.62		
Patsio, Lahaul Spiti, Western Himalaya	Range	5.66 – 7.02	11.25 – 12.41	5.39 – 5.59	µg C $g^{-1}day^{-1}$	Present study
	Mean ± SD	6.34 ± 0.96	11.83 ± 0.82	5.49 ± 0.14		
Antarctica Blue-ice area, East Antarctic Ice Sheet (mean values of 11 sites)	Mean	0.23	2.23	2.00	µg C $g^{-1}day^{-1}$	(Hodson et al. 2013)
Midtre Lovénbreen, Vestre Brøggerbreen and Austre Brøggerbreen, Svalbard	Mean ± SD	-0.12 ± 4.10	18.70 ± 10.30	18.70 ± 9.10	µg C $g^{-1}day^{-1}$	(Telling et al. 2012)

Leverett Glacier, Greenland Ice Sheet (mean values from 9 sites along a transect)	Mean	6.11	24.51	18.40	µg C $g^{-1}day^{-1}$	(Stibal et al. 2012b)
Midtre Lovénbreen, Svalbard	Mean	-20*	17.20 ± 9.70	19.20 ± 5.50	µg C $g^{-1}day^{-1}$	(Hodson et al. 2010b)
Greenland Ice Sheet (southwest)	Mean	-2.20*	18.70 ± 10.10	20.90 ± 8.20	µg C $g^{-1}day^{-1}$	(Hodson et al. 2010b)
East Antarctic ice sheet (Vestfold Hills)	Mean	0.24*	2.10 ± 1.50	1.86 ± 1.51	µg C $g^{-1}day^{-1}$	(Hodson et al. 2010b)

(*NEP value was calculated from the mean differences of P and R reported in the respective study)

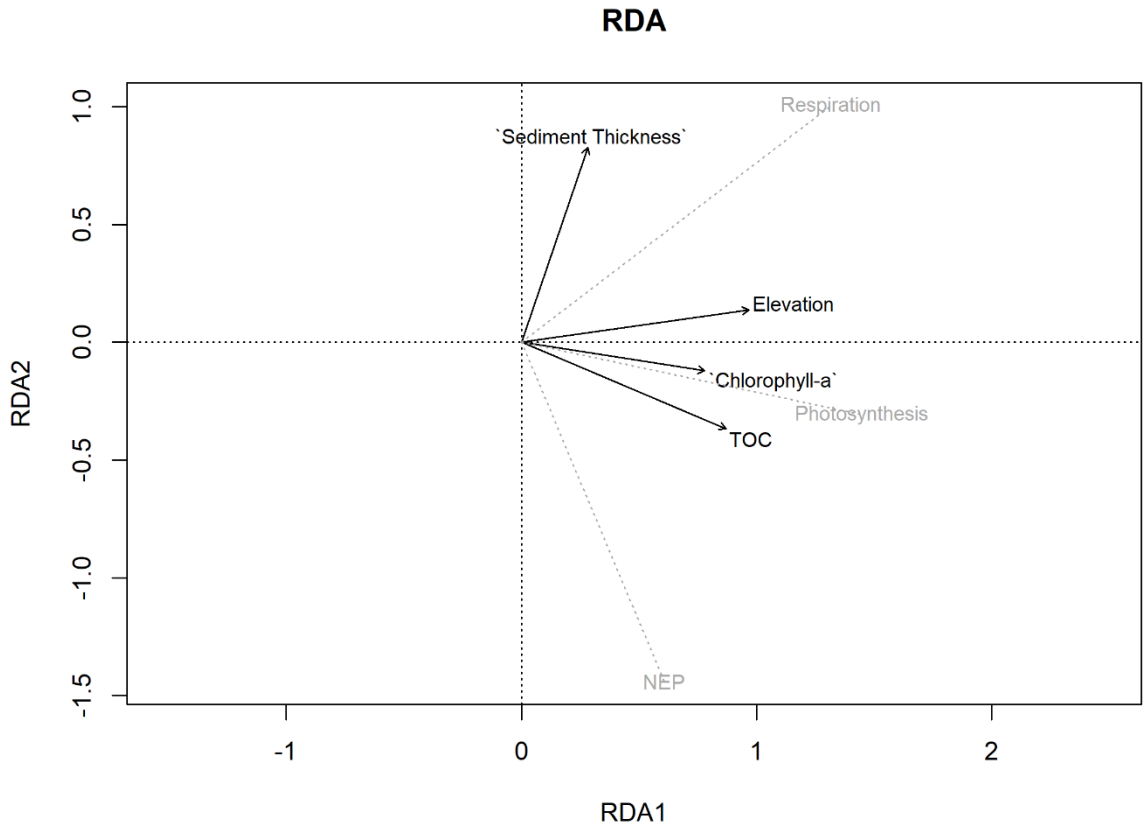

Fig. 7 Result of RDA plot of the explanatory variables (sediment thickness, elevation, chlorophyll-*a* and TOC) with Respiration, Photosynthesis and NEP as the dependent variables. The significant level of the explanatory variables is at <0.05

373

374 **Table 6** Result of the RDA using manual forward selection, with dependent variables as Photosynthesis,

375 Respiration and NEP

376

	Percentage of Variance (%)	F value	p-value
Photosynthesis	82.3		
Chlorophyll-*a*	39.6	15.7	0.009
TOC	24.6	9.7	0.023
Elevation	16.3	6.5	0.041
Respiration	95.1		
Sediment Thickness	37.1	53.7	0.001
Elevation	33.1	47.9	0.001
Chlorophyll-*a*	24.8	36.0	0.002
NEP	74.2		
TOC	35.8	9.7	0.021
Sediment Thickness	22.1	6.0	0.040

377

378 **4.2. Sources of organic matter in the Western Himalaya**

379 Since most research into glacier surface biological productivity is conducted in the Polar Regions, studies in the
380 Himalayan region are very limited. Telling et al. (2012) from their earlier studies on Arctic glaciers proposed three
381 possible sources for enhanced organic carbon content in glacier cryoconite. First, it may arise from long-distance
382 deposition of rich organic carbon from outside the glacier to the cryoconite holes. Second, it may reflect
383 autochthonously produced organic carbon in supraglacial habitats and re-deposited into cryoconite holes. Third,
384 it may be due to very high NEP rates within cryoconite holes under favourable environmental settings such as
385 thin sediment layers (Telling et al. 2012) or lateral thermal expansion of cryoconite holes, following maximum
386 exposure of the cryoconite to solar radiation (Cook et al. 2010) which may result in greater organic matter
387 production within the holes. In order to evaluate the potential organic matter accumulation mechanisms, here we
388 estimate using our experimental data, the number of melt seasons it would take for organic matter and phototrophic
389 biomass to accumulate in cryoconite holes at our two Himalayan glacier sites.

The total number of melt seasons required to generate the observed TOC content (µg C per g^{-1} sediment) of our cryoconite samples was assessed in a similar manner to Telling et al. (2012), as follows:

$$Melt\ seasons = \frac{Total\ Carbon\ content\ of\ cryoconite}{NEP \times melt\ time} \quad (2)$$

Here, Total Carbon (TC) of the cryoconite (µg C g^{-1} dry sediment) was taken to be approximately equal to the TOC content. Only samples with net autotrophic NEP values (µg C g^{-1} day^{-1}) were considered for the calculation. The melt time is the typical duration of the melt season, which we assumed as 124 ± 13 days (mid-May – mid-September) for Western Himalayan glaciers as estimated by Panday et al. (2011). The number of melt seasons required to accumulate phototroph biomass was also calculated in a similar manner using Eq. (2), by substituting TC content for phototrophic biomass. Phototrophic biomass was estimated using a ratio of 1:47 between the chlorophyll-*a* concentration of cryoconite and the TOC content based on the estimation in phytoplankton species by Riemann et al. (1989). However, this estimation may not take into account all the extracellular polymers produced by autotrophs, as cryoconite may have a much higher ratio of organic carbon to chlorophyll-*a* (Telling et al. 2010). Caution must be exercised in interpreting these data, since the experiment performed was a snapshot study (done just for 24 hours) in the ablation period only, and could not account for the rate of migration of the cryoconite particles, oxygenation and pH profiles within the cryoconite layer.

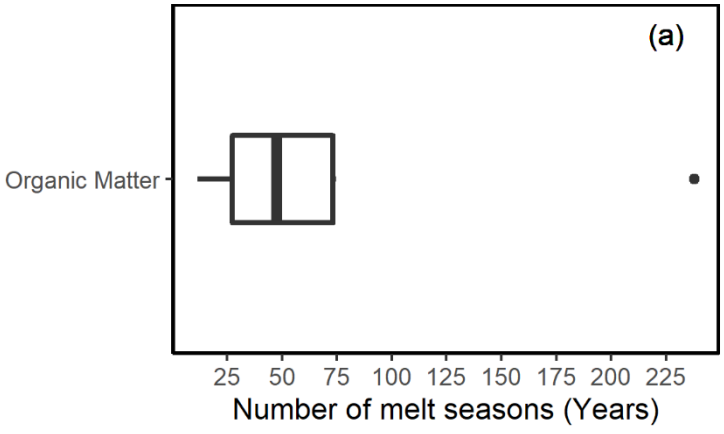

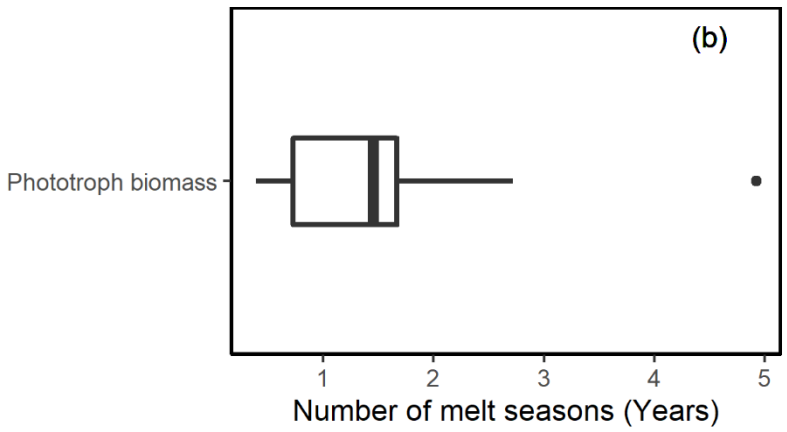

Fig. 8 Boxplots showing the estimated number of melt seasons (in years) required to produce (a) organic carbon (mean = 68 years, max= 74 years (one outlier 237 years), min = 11 years, Q1 = 27 years, Q3= 73 years) and (b) phototroph biomass (mean= 1.7 years, max =3 (one outlier 5 years), min = 0.4 year, Q1 = 0.7 year, Q3 = 2 year) in the cryoconite holes

We estimate that the average time to form a thin layer of autotrophic biomass (approx. < 0.3 cm) on the glacier surface is 1.7 ± 1.5 years (with a range of 4 months - 3 years, with an outlier of 5 years) (Fig. 8). Within the same cryoconite hole, the average time required for organic carbon accumulation to account for the measured carbon contents is 68 years (range 11 – 74 years, with an outlier of 238 years) (Fig.8). The above calculations show that during the *in situ* experimental periods, the overall net autochthonously produced organic carbon inside the cryoconite holes could not explain most of the accumulated organic content. The age of hydrologically connected cryoconite holes on the Chhota Shigri and Patsio glaciers is unknown. In Svalbard valley glaciers, it is estimated that the typical age of cryoconite is between >1 year and several years, (Stibal et al. 2008). Hydrologically isolated cryoconite holes like those on the Greenland Ice Sheet, however, may have a lifetime of >100 years and will be in a position to produce and accumulate organic matter better via autochthonous processes (Hodson et al. 2010a; Stibal et al. 2012a). In contrast much older carbon (6 – 10 ky) is found to accumulate over time in ice-lidded cryoconite holes on the Antarctic Ice Sheet which might be isolated from the atmosphere for much longer periods (Lutz et al. 2019). Compared to polar regions, cryoconite holes in the Himalaya are shallower and have a shorter life span due to high melt rates (Takeuchi et al. 2000), therefore more frequent redistribution of the cryoconite across ice surfaces might be expected. This may explain the lower rates of Respiration and Photosynthesis observed in our studied cryoconite holes compared to Arctic glaciers and the Greenland Ice Sheets (Table 5). Since the cryoconite holes in the Himalayas are formed quickly and generally do not last long, most of the carbon inside the cryoconite hole most likely either reflects allochthonous deposition, or biologically produced organic

carbon formed elsewhere on the glacier surface, for example, in surface ice via glacier algae (Tranter et al. 2004; Telling et al. 2012; Stibal et al. 2012a). We examine the potential source of the organic carbon and phototroph biomass below.

In the Himalaya, long-distance transportation and deposition of allochthonous organic carbon have been observed on snow and ice surfaces (Xu et al. 2013; Niu et al. 2017; Zhang et al. 2018). The Western Himalayan region, because of its remote position, is less influenced by long-distance transportation, therefore most supraglacial carbon content has been inferred to originate from *in situ* biological processes by photoautotrophic and heterotrophic activity, and deposition of carbon, derived locally from biomass burning of C3 vegetation (Nizam et al. 2020). Another source of organic matter in the Himalayan supraglacial environment is that from snow and ice algal communities (Yoshimura et al. 1997, 2000). Various diverse microbial communities, such as cyanobacteria, fungi, and plankton, thrive in snow, moraine lakes and stream water of Himalaya (Liu et al. 2011; Kammerlander et al. 2015; Sanyal et al. 2018; Azzoni et al. 2018) could be potential organic carbon sources in the region. An abundance of phototrophic cyanobacteria such as microcoleus and oscillatoriales has been reported in cryoconite from Asian glaciers during the later melt season (Segawa et al. 2017). On the Greenland Ice Sheet, snow and ice algae constitute a majority of the supraglacial microbial community and dominate the net primary production after the onset of melt season (Yallop et al. 2012; Lutz et al. 2014; Stibal et al. 2017; Williamson et al. 2018, 2019, 2021). This algal biomass retained on glacier ice surfaces has the potential to sustain cryoconite holes by providing organic carbon and nutrients to other microbial communities (Tranter et al. 2004; Wadham et al. 2010; Antony et al. 2014; Lutz et al. 2015; Williamson et al. 2018). Additionally, secondary heterotrophs surviving on glacier surfaces may further modify the organic carbon deposited thereby producing complex organic carbon through *in situ* processes (Sanyal et al. 2018; Nizam et al. 2020). Considering the estimated time taken to produce organic carbon (average ~68 years) on our study glaciers, and the inferred short life of cryoconite holes in the Himalaya (Takeuchi et al. 2000), we infer that a significant proportion of the organic carbon in cryoconite might originate outside of cryoconite holes through surface ice microbial production redistributed in the supraglacial environment and incorporated with the freshly formed cryoconite holes or from vegetation biomass redistributed by wind (Nizam et al. 2020). This interpretation would reconcile our lengthy times for cryoconite TOC to accumulate and support the recent finding from biomarker and geochemical tracers ($\delta^{13}C$, Pb isotopes) that TOC in cryoconite holes in the Western Himalaya has a strong biological origin (Nizam et al. 2020).

4.3. Future Implications

Potential microbial activity on the surfaces of two largely debris-free Himalayan glaciers has been revealed for the first time through *in situ* NEP and Respiration measurements. Our study provides a significant first step in evaluating the potential influence of biological activity on the physical behaviour of the glaciers in Himalaya. Since Himalayan glaciers share a similar climatic environment to that of the Polar Regions, biological activity observed on Himalayan glacier surfaces might also play a significant role in driving the glacier melting by absorbing summer solar energy. The organic matter accumulated on the glacier surface, through primary production, may lead to a positive feedback on glacier melting (the so called "bio-albedo" effect) (Takeuchi et al. 2000; Lutz et al. 2014; Cook et al. 2017; Hotaling et al. 2021). Although glacier mass loss due to the bio-albedo effect is not well quantified, a study by Williamson et al. (2020) reported that glacier algae may be responsible for up to 75 % of the variability in albedo in the Southwestern Greenland Ice Sheet. While ice algae are important in surface albedo reduction on an ice sheet scale (Yallop et al. 2012; Lutz et al. 2014; Stibal et al. 2017; Williamson et al. 2018; Tedstone et al. 2019), the importance of ice algae on valley glaciers like Himalayan glaciers are unclear. It is, therefore, important to focus on the microbial communities both on the ice surfaces as well as cryoconite holes further in future. Apart from the potential physical changes on glacial surfaces due to microbial activity, the organic matter deposited on the glacier surface within cryoconite holes and dispersed on the glacier surface may result in the export of dissolved organic matter and nutrients to downstream ecosystems, thereby changing the activity and function of the recipient microbial community. Therefore, in light of the important ecosystem processes carried out in this extreme environment, future research on Himalayan glaciers should incorporate the potential role of microbial activity on the glacier mass loss and its possible implications for downstream ecosystem.

5. Conclusion

Potential microbial activity in the cryoconite holes of two largely debris-free Western Himalayan glacier surfaces, Chhota Shigri and Patsio glaciers, was measured for the first time. Diverse microbial and environmental variables including organic matter content, chlorophyll-*a*, altitude, grain size and stability of the cryoconite were studied to identify and understand the factors controlling the NEP. A significant association between organic matter (TOC % and TN %) with chlorophyll-*a* content ($r = 0.94$ and 0.95 respectively = 10, $p < 0.05$) and a general increase in the fine mineral fraction of cryoconite from lower and middle to the upper sites in Chhota Shigri glacier was observed. Net positive autotrophy dominated the cryoconite holes in the upper ablation region at Chhota Shigri

and at Patsio glacier, which hosts relatively stable cryoconite holes with a relatively high chlorophyll-*a* content. The latter enables microbial communities to carry out photosynthesis in the supraglacial environment of the Himalaya. Net heterotrophy associated with coarser grain sizes, reduced organic matter and chlorophyll-*a* content was observed in the lower ablation zone, which potentially reflects the disturbance of cryoconite holes by frequent flushing by meltwater channels. Multivariate statistical analysis using RDA indicated that sediment thicknesses were a significant factor controlling the rate of Respiration (37.1 %; df = 1, F value = 53.7, p = 0.001) in cryoconite holes in Chhota Shigri. Chlorophyll-*a* content of the cryoconite holes significantly controlled the rate of Photosynthesis (39.6 %; df = 1, F value = 15.7, p = 0.009). While the rate of NEP were significantly controlled by the TOC content and sediment thickness of cryoconite holes (35.8 % ; df = 1, F value = 9.7, p = 0.021 and 22.1 %; df = 1, F value = 6.0, p = 0.04) of the total variance in the experiments performed in a limited time. Phototrophic biomass in the cryoconite holes (sediment thickness <3 cm) was estimated to take 1.7 ± 1.5 years to accumulate, supporting its production via autochthonous processes on the glacier surface. However, the organic carbon in the same cryoconite holes took an estimated 11 to 70 years to form, indicating that allochthonous and/or autochthonous organic carbon formed elsewhere on the glacier surface, such as in surface ice, may contribute to the accumulation of organic carbon in cryoconite holes.

Acknowledgements

This research was funded by “Bio-climatic feedbacks of melting Himalayan ice” (UKIERI: UK-India Research and Education Initiative to Wadham and Ramanathan) (DST/INT/UK/P-140/2016). The authors gratefully acknowledge the staff members of LOWTEX laboratory, University of Bristol, UK for providing facilities to analyse the samples. The authors also like to thank the Glaciological groups of Jawaharlal Nehru University and the University of Bristol for their support during the fieldwork.

Reference:

Anesio AM, Hodson AJ, Fritz A, et al (2009) High microbial activity on glaciers: Importance to the global carbon cycle. Glob Chang Biol 15:955–960. https://doi.org/10.1111/j.1365-2486.2008.01758.x

Angchuk T (2020) Glacio-meteorological and hydrological studies of Patsio Glacier, Himachal pradesh, Western Himalaya. PhD Thesis JNU, New Delhi

Angchuk T, Ramanathan A, Bahuguna IM, et al (2021) Annual and seasonal glaciological mass balance of Patsio Glacier, western Himalaya (India) from 2010 to 2017. J Glaciol 67:1137–1146. https://doi.org/10.1017/JOG.2021.60

Antony R, Grannas AM, Willoughby AS, et al (2014) Origin and sources of dissolved organic matter in snow on the east antarctic ice sheet. Environ Sci Technol 48:6151–6159. https://doi.org/10.1021/es405246a

Azam MF, Wagnon P, Patrick C, et al (2014a) Reconstruction of the annual mass balance of Chhota Shigri glacier, Western Himalaya, India, since 1969. Ann Glaciol 55:69–80. https://doi.org/10.3189/2014AoG66A104

Azam MF, Wagnon P, Vincent C, et al (2014b) Processes governing the mass balance of Chhota Shigri Glacier (western Himalaya, India) assessed by point-scale surface energy balance measurements. Cryosphere 8:2195–2217. https://doi.org/10.5194/tc-8-2195-2014

Azzoni RS, Tagliaferri I, Franzetti A, et al (2018) Bacterial diversity in snow from mid-latitude mountain areas: Alps, Eastern Anatolia, Karakoram and Himalaya. Ann Glaciol 59:10–20. https://doi.org/10.1017/aog.2018.18

Bagshaw, EA, Tranter, M, Fountain, AG, et al (2013) Do Cryoconite Holes have the Potential to be Significant Sources of C, N, and P to Downstream Depauperate Ecosystems of Taylor Valley, Antarctica? Arctic, Antarct Alp Res 45:440–454. https://doi.org/10.1657/1938-4246-45.4.440

Bagshaw EA, Tranter M, Wadham JL, et al (2016) Processes controlling carbon cycling in Antarctic glacier surface ecosystems. Geochemical Perspect Lett 2:44–54. https://doi.org/10.7185/geochemlet.1605

Bakke J, Vasskog K, Ramanathan A, et al (2016) The Water Tower of India in a Long-term Perspective – A Way to Reconstruct Glaciers and Climate in Himachal Pradesh during the last 13,000 Years. J Clim Chang 2:103–112. https://doi.org/10.3233/jcc-160011

Bolch T, Kulkarni A, Kääb A, et al (2012) The state and fate of himalayan glaciers. Science (80-.). 336:310–314

Bolch T, Shea JM, Liu S, et al (2019) Status and Change of the Cryosphere in the Extended Hindu Kush Himalaya Region. In: The Hindu Kush Himalaya Assessment. Springer International Publishing, pp 209–255

Borcard D, Gillet F, Legendre P (2011) Numerical Ecology with R. Springer New York

Buda J, Poniecka EA, Rozwalak P, et al (2021) Is Oxygenation Related to the Decomposition of Organic Matter in Cryoconite Holes? Ecosystems 1–12. https://doi.org/10.1007/s10021-021-00729-2

Chandler DM, Alcock JD, Wadham JL, et al (2015) Seasonal changes of ice surface characteristics and productivity in the ablation zone of the Greenland Ice Sheet. Cryosphere 9:487–504. https://doi.org/10.5194/tc-9-487-2015

Cook J, Hodson A, Telling J, et al (2010) The mass–area relationship within cryoconite holes and its implications for primary production. Ann Glaciol 51:106–110. https://doi.org/10.3189/172756411795932038

Cook JM, Hodson AJ, Gardner AS, et al (2017) Quantifying bioalbedo: A new physically-based model and critique of empirical methods for characterizing biological influence on ice and snow albedo. Cryosph Discuss 1–29. https://doi.org/10.5194/tc-2017-73

Cook JM, Sweet M, Cavalli O, et al (2018) Topographic shading influences cryoconite morphodynamics and carbon exchange. https://doi.org/101080/1523043020171414463 50:. https://doi.org/10.1080/15230430.2017.1414463

Edwards A, Anesio AM, Rassner SM, et al (2011) Possible interactions between bacterial diversity, microbial activity and supraglacial hydrology of cryoconite holes in Svalbard. ISME J 5:150–160. https://doi.org/10.1038/ismej.2010.100

Fagerbakke KM, Heldal M, Norland S (1996) Content of carbon, nitrogen, oxygen, sulfur and phosphorus in native aquatic and cultured bacteria. Aquat Microb Ecol 10:15–27. https://doi.org/10.3354/ame010015

Foreman CM, Sattler B, Mikucki JA, et al (2007) Metabolic activity and diversity of cryoconites in the Taylor Valley, Antarctica. J Geophys Res Biogeosciences 112:n/a-n/a. https://doi.org/10.1029/2006JG000358

Fountain AG, Tranter M, Nylen TH, et al (2004) Evolution of cryoconite holes and their contribution to meltwater runoff from glaciers in the McMurdo Dry Valleys, Antarctica. J Glaciol 50:35–45. https://doi.org/10.3189/172756504781830312

Fujita K, Nuimura T (2011) Spatially heterogeneous wastage of Himalayan glaciers. Proc Natl Acad Sci U S A 108:14011–14014. https://doi.org/10.1073/pnas.1106242108

Garg PK, Shukla A, Tiwari RK, Jasrotia AS (2017) Assessing the status of glaciers in part of the Chandra basin, Himachal HimalayaA multiparametric approach. Geomorphology 284:99–114. https://doi.org/10.1016/j.geomorph.2016.10.022

Garg S, Shukla A, Garg PK, et al (2021) Revisiting the 24 year (1994-2018) record of glacier mass budget in the Suru sub-basin, western Himalaya: Overall response and controlling factors. Sci Total Environ 800:.

https://doi.org/10.1016/j.scitotenv.2021.149533

Higgins SA, Overeem I, Rogers KG, Kalina EA (2018) River linking in India: Downstream impacts on water discharge and suspended sediment transport to deltas. Elementa 6:. https://doi.org/10.1525/elementa.269

Hodson A, Anesio AM, Ng F, et al (2007) A glacier respires: Quantifying the distribution and respiration CO2 flux of cryoconite across an entire arctic supraglacial ecosystem. J Geophys Res Biogeosciences 112:. https://doi.org/10.1029/2007JG000452

Hodson A, Bøggild C, Hanna E, et al (2010a) The cryoconite ecosystem on the Greenland ice sheet. Ann Glaciol 51:123–129. https://doi.org/10.3189/172756411795931985

Hodson A, Cameron K, Bøggild C, et al (2010b) The structure, biological activity and biogeochemistry of cryoconite aggregates upon an Arctic valley glacier: Longyearbreen, Svalbard. J Glaciol 56:349–362

Hodson A, Paterson H, Westwood K, et al (2013) A blue-ice ecosystem on the margins of the East Antarctic ice sheet. J Glaciol 59:255–268. https://doi.org/10.3189/2013JoG12J052

Hodson AJ, Mumford PN, Kohler J, Wynn PM (2005) The High Arctic glacial ecosystem: New insights from nutrient budgets. Biogeochemistry 72:233–256. https://doi.org/10.1007/s10533-004-0362-0

Holland AT, Williamson CJ, Sgouridis F, et al (2019) Dissolved organic nutrients dominate melting surface ice of the Dark Zone (Greenland Ice Sheet). Biogeosciences 16:3283–3296. https://doi.org/10.5194/bg-16-3283-2019

Hotaling S, Lutz S, Dial RJ, et al (2021) Biological albedo reduction on ice sheets, glaciers, and snowfields. Earth-Science Rev. 220:103728

Kammerlander B, Breiner HW, Filker S, et al (2015) High diversity of protistan plankton communities in remote high mountain lakes in the European Alps and the Himalayan mountains. FEMS Microbiol Ecol 91:. https://doi.org/10.1093/femsec/fiv010

Kastovská K, Elster J, Stibal M, Santrůcková H (2005) Microbial assemblages in soil microbial succession after glacial retreat in Svalbard (high arctic). Microb Ecol 50:396–407. https://doi.org/10.1007/s00248-005-0246-4

Kohshima S, Yoshimura Y, Takeuchi N (2002) Glacier Ecosystem and Biological ICE-Core Analysis. pp 1–8

Kumari S, Pandit A, Ramsankaran R, et al (2021) Modelling ice thickness distribution and volume of Patsio Glacier in Western Himalayas. J Earth Syst Sci 130:1–14. https://doi.org/10.1007/s12040-021-01643-w

Langford HJ, Irvine-Fynn TDL, Edwards A, et al (2014) A spatial investigation of the environmental controls over cryoconite aggregation on Longyearbreen glacier, Svalbard. Biogeosciences 11:5365–5380.

https://doi.org/10.5194/bg-11-5365-2014

Lee E, Carrivick JL, Quincey DJ, et al (2021) Accelerated mass loss of Himalayan glaciers since the Little Ice Age. Sci Rep 11:1–8. https://doi.org/10.1038/s41598-021-03805-8

Leidman SZ, Rennermalm ÅK, Muthyala R, et al (2021) The Presence and Widespread Distribution of Dark Sediment in Greenland Ice Sheet Supraglacial Streams Implies Substantial Impact of Microbial Communities on Sediment Deposition and Albedo. Geophys. Res. Lett. 48:2020GL088444

Liu Y, Yao T, Jiao N, et al (2011) Microbial diversity in the snow, a moraine lake and a stream in Himalayan glacier. Extremophiles 15:411–421. https://doi.org/10.1007/s00792-011-0372-5

Lorenzen CJ (1967) DETERMINATION OF CHLOROPHYLL AND PHEO-PIGMENTS: SPECTROPHOTOMETRIC EQUATIONS. Limnol. Oceanogr. 12:343–346

Lutz S, Anesio AM, Edwards A, Benning LG (2017) Linking microbial diversity and functionality of arctic glacial surface habitats. Environ Microbiol 19:551–565. https://doi.org/10.1111/1462-2920.13494

Lutz S, Anesio AM, Edwards A, Benning LG (2015) Microbial diversity on icelandic glaciers and ice caps. Front Microbiol 6:. https://doi.org/10.3389/fmicb.2015.00307

Lutz S, Anesio AM, Jorge Villar SE, Benning LG (2014) Variations of algal communities cause darkening of a Greenland glacier. FEMS Microbiol Ecol 89:402–414. https://doi.org/10.1111/1574-6941.12351

Lutz S, Ziolkowski LA, Benning LG (2019) The biodiversity and geochemistry of cryoconite holes in queen maud land, East Antarctica. Microorganisms 7:. https://doi.org/10.3390/microorganisms7060160

MacDonell SA, Fitzsimons SJ (2012) Observations of cryoconite hole system processes on an Antarctic glacier. Rev Chil Hist Nat 85:393–407. https://doi.org/10.4067/S0716-078X2012000400003

Mandal A, Ramanathan A, Angchuk T, et al (2016) Unsteady state of glaciers (Chhota Shigri and Hamtah) and climate in Lahaul and Spiti region, western Himalayas: a review of recent mass loss. Environ Earth Sci 75:. https://doi.org/10.1007/s12665-016-6023-5

Mandal A, Ramanathan A, Azam MF, et al (2020) Understanding the interrelationships among mass balance, meteorology, discharge and surface velocity on Chhota Shigri Glacier over 2002-2019 using in situ measurements. J Glaciol 66:727–741. https://doi.org/10.1017/jog.2020.42

Maurer JM, Schaefer JM, Rupper S, Corley A (2019) Acceleration of ice loss across the Himalayas over the past 40 years. 5:eaav7266

Musilova M, Tranter M, Bamber JLL, et al (2016) Experimental evidence that microbial activity lowers the albedo of glaciers. Geochemical Perspect Lett 2:106–116. https://doi.org/10.7185/geochemlet.1611

Nicholes MJ, Williamson CJ, Tranter M, et al (2019) Bacterial dynamics in supraglacial habitats of the Greenland ice sheet. Front Microbiol 10:1366. https://doi.org/10.3389/fmicb.2019.01366

Niu H, Kang S, Shi X, et al (2017) In-situ measurements of light-absorbing impurities in snow of glacier on Mt. Yulong and implications for radiative forcing estimates. Sci Total Environ. https://doi.org/10.1016/j.scitotenv.2017.01.032

Nizam S, Sen IS, Vinoj V, et al (2020) Biomass-Derived Provenance Dominates Glacial Surface Organic Carbon in the Western Himalaya. Environ Sci Technol 54:8612–8621. https://doi.org/10.1021/acs.est.0c02710

Panday PK, Frey KE, Ghimire B (2011) Detection of the timing and duration of snowmelt in the Hindu Kush-Himalaya using QuikSCAT, 2000–2008. Environ Res Lett 6:24007–24020. https://doi.org/10.1088/1748-9326/6/2/024007

Pittino F, Maglio M, Gandolfi I, et al (2018) Bacterial communities of cryoconite holes of a temperate alpine glacier show both seasonal trends and year-to-year variability. Ann Glaciol 59:1–9. https://doi.org/10.1017/aog.2018.16

Poniecka EA, Bagshaw EA, Tranter M, et al (2018) Rapid development of anoxic niches in supraglacial ecosystems. Arctic, Antarct Alp Res 50:. https://doi.org/10.1080/15230430.2017.1420859

Pritchard HD (2017) Asia's glaciers are a regionally important buffer against drought. Nature 545:169–174

Qian Y, Yasunari TJ, Doherty SJ, et al (2015) Light-absorbing Particles in Snow and Ice: Measurement and Modeling of Climatic and Hydrological impact. Adv Atmos Sci. https://doi.org/10.1007/s00376-014-0010-0

Remias D, Lütz-Meindl U, Lütz C (2005) Photosynthesis, pigments and ultrastructure of the alpine snow alga Chlamydomonas nivalis. Eur J Phycol 40:259–268. https://doi.org/10.1080/09670260500202148

Riemann B, Simonsen P, Stensgaard L (1989) The carbon and chlorophyll content of phytoplankton from various nutrient regimes. J Plankton Res 11:1037–1045. https://doi.org/10.1093/plankt/11.5.1037

Rounce DR, Hock R, Shean DE (2020) Glacier Mass Change in High Mountain Asia Through 2100 Using the Open-Source Python Glacier Evolution Model (PyGEM). Front Earth Sci 7:331. https://doi.org/10.3389/feart.2019.00331

Rozwalak P, Podkowa P, Buda J, et al (2022) Cryoconite – From minerals and organic matter to bioengineered sediments on glacier's surfaces. Sci Total Environ 807:150874. https://doi.org/10.1016/j.scitotenv.2021.150874

Samui G, Antony R, Thamban M (2018) Chemical characteristics of hydrologically distinct cryoconite holes in

665 coastal Antarctica. Ann Glaciol 59:69–76. https://doi.org/10.1017/aog.2018.30
666 Sanyal A, Antony R, Samui G, Thamban M (2018) Microbial communities and their potential for degradation of
667 dissolved organic carbon in cryoconite hole environments of Himalaya and Antarctica. Microbiol Res
668 208:32–42. https://doi.org/10.1016/j.micres.2018.01.004
669 Säwström C, Mumford P, Marshall W, et al (2002) The microbial communities and primary productivity of
670 cryoconite holes in an Arctic glacier (Svalbard 79°N). Polar Biol 25:591–596.
671 https://doi.org/10.1007/s00300-002-0388-5
672 Segawa T, Yonezawa T, Edwards A, et al (2017) Biogeography of cryoconite forming cyanobacteria on polar and
673 Asian glaciers. J Biogeogr 44:2849–2861. https://doi.org/10.1111/jbi.13089
674 Stibal M, Box JE, Cameron KA, et al (2017) Algae Drive Enhanced Darkening of Bare Ice on the Greenland Ice
675 Sheet. Geophys Res Lett 44:11,463-11,471. https://doi.org/10.1002/2017GL075958
676 Stibal M, Lawson EC, Lis GP, et al (2010) Organic matter content and quality in supraglacial debris across the
677 ablation zone of the Greenland ice sheet. Ann Glaciol 51:1–8.
678 https://doi.org/10.3189/172756411795931958
679 Stibal M, Šabacká M, Kaštovská K (2006) Microbial communities on glacier surfaces in Svalbard: Impact of
680 physical and chemical properties on abundance and structure of cyanobacteria and algae. Microb Ecol
681 52:644–654. https://doi.org/10.1007/s00248-006-9083-3
682 Stibal M, Šabacká M, Žárský J (2012a) Biological processes on glacier and ice sheet surfaces. Nat Geosci 5:771–
683 774. https://doi.org/10.1038/ngeo1611
684 Stibal M, Telling J, Cook J, et al (2012b) Environmental Controls on Microbial Abundance and Activity on the
685 Greenland Ice Sheet: A Multivariate Analysis Approach. Microb Ecol 63:74–84.
686 https://doi.org/10.1007/s00248-011-9935-3
687 Stibal M, Tranter M, Benning LG, Řehák J (2008) Microbial primary production on an Arctic glacier is
688 insignificant in comparison with allochthonous organic carbon input. Environ Microbiol 10:2172–2178.
689 https://doi.org/10.1111/j.1462-2920.2008.01620.x
690 Takeuchi N (2002) Optical characteristics of cryoconite (surface dust) on glaciers: The relationships between light
691 absorbency and the property of organic matter contained in the cryoconite. Ann Glaciol 34:409–414.
692 https://doi.org/10.3189/172756402781817743
693 Takeuchi N (2013) Seasonal and altitudinal variations in snow algal communities on an Alaskan glacier (Gulkana
694 glacier in the Alaska range). Environ Res Lett 8:. https://doi.org/10.1088/1748-9326/8/3/035002

Takeuchi N, Dial R, Kohshima S, et al (2006) Spatial distribution and abundance of red snow algae on the Harding Icefield, Alaska derived from a satellite image. Geophys Res Lett 33:. https://doi.org/10.1029/2006GL027819

Takeuchi N, Kohshima S, Seko K (2001) Structure, Formation, and Darkening Process of Albedo-reducing Material (Cryoconite) on a Himalayan Glacier: A Granular Algal Mat Growing on the Glacier. Arctic, Antarct Alp Res 33:115–122. https://doi.org/10.1080/15230430.2001.12003413

Takeuchi N, Kohshima S, Yoshimura Y, et al (2000) Characteristics of cryoconite holes on a Himalayan glacier, Yala Glacier Central Nepal. Bull Glaciol Res 17:51–59

Takeuchi N, Nishiyama H, Li Z (2010) Structure and formation process of cryoconite granules on ürümqi glacier No. 1, Tien Shan, China. Ann Glaciol 51:9–14. https://doi.org/10.3189/172756411795932010

Tedstone A, Cook J, Williamson C, et al (2019) Algal growth and weathering crust structure drive variability in Greenland Ice Sheet ice albedo. Cryosph Discuss 1–24. https://doi.org/10.5194/tc-2019-131

Telling J, Anesio AM, Tranter M, et al (2012) Controls on the autochthonous production and respiration of organic matter in cryoconite holes on high Arctic glaciers. J Geophys Res Biogeosciences 117:1017. https://doi.org/10.1029/2011JG001828

Telling J, Anesio AMM, Hawkings J, et al (2010) Measuring rates of gross photosynthesis and net community production in cryoconite holes: a comparison of field methods

Tranter M, Fountain AG, Fritsen CH, et al (2004) Extreme hydrochemical conditions in natural microcosms entombed within Antarctic ice. Hydrol Process 18:379–387. https://doi.org/10.1002/hyp.5217

Uetake J, Naganuma T, Hebsgaard MB, et al (2010) Communities of algae and cyanobacteria on glaciers in west Greenland. Polar Sci 4:71–80. https://doi.org/10.1016/j.polar.2010.03.002

Wadham JL, Tranter M, Skidmore M, et al (2010) Biogeochemical weathering under ice: Size matters. Global Biogeochem Cycles 24:n/a-n/a. https://doi.org/10.1029/2009GB003688

Williamson CJ, Anesio AM, Cook J, et al (2018) Ice algal bloom development on the surface of the Greenland Ice Sheet. FEMS Microbiol Ecol 94:1–10. https://doi.org/10.1093/femsec/fiy025

Williamson CJ, Cameron KA, Cook JM, et al (2019) Glacier Algae: A Dark Past and a Darker Future. Front Microbiol 10:524. https://doi.org/10.3389/fmicb.2019.00524

Williamson CJ, Cook J, Tedstone A, et al (2020) Algal photophysiology drives darkening and melt of the Greenland Ice Sheet. 117:5694–5705

Williamson CJ, Turpin-Jelfs T, Nicholes MJ, et al (2021) Macro-Nutrient Stoichiometry of Glacier Algae From

the Southwestern Margin of the Greenland Ice Sheet. Front Plant Sci 12:911

Xu J, Zhang Q, Li X, et al (2013) Dissolved organic matter and inorganic ions in a central himalayan glacier - insights into chemical composition and atmospheric sources. Environ Sci Technol 47:6181–6188. https://doi.org/10.1021/es4009882

Yallop ML, Anesio AM, Perkins RG, et al (2012) Photophysiology and albedo-changing potential of the ice algal community on the surface of the Greenland ice sheet. ISME J 6:2302–2313. https://doi.org/10.1038/ismej.2012.107

Yoshimura Y, Kohshima S, Ohtani S (1997) A Community of Snow Algae on a Himalayan Glacier: Change of Algal Biomass and Community Structure with Altitude. Arct Alp Res. https://doi.org/10.1080/00040851.1997.12003222

Yoshimura Y, Kohshima S, Takeuchi N, et al (2000) Himalayan ice-core dating with snow algae. J Glaciol. https://doi.org/10.3189/172756500781832918

Zarsky JD, Stibal M, Hodson A, et al (2013) Large cryoconite aggregates on a Svalbard glacier support a diverse microbial community including ammonia-oxidizing archaea. Environ Res Lett 8:035044. https://doi.org/10.1088/1748-9326/8/3/035044

Zawierucha K, Porazinska DL, Ficetola GF, et al (2021) A hole in the nematosphere: tardigrades and rotifers dominate the cryoconite hole environment, whereas nematodes are missing. J Zool 313:18–36. https://doi.org/10.1111/jzo.12832

Zhang Y, Xu M, Li X, et al (2018) Hydrochemical characteristics and multivariate statistical analysis of natural water system: A case study in Kangding County, Southwestern China. Water (Switzerland) 10:80. https://doi.org/10.3390/w10010080

Zhao H, Yang W, Yao T, et al (2016) Dramatic mass loss in extreme high-elevation areas of a western Himalayan glacier: Observations and modeling. Sci Rep 6:. https://doi.org/10.1038/srep30706

Zhao L, Ding R, Moore JC (2014) Glacier volume and area change by 2050 in high mountain Asia. Glob Planet Change 122:197–207. https://doi.org/10.1016/j.gloplacha.2014.08.006

Statements and Declarations

Funding

This work was supported by UKIERI-DST partnership, “Bio-climatic feedbacks of melting Himalayan ice” (UKIERI: UK-India Research and Education Initiative to Wadham and Ramanathan) (DST/INT/UK/P-140/2016).

The author MSS also received research support through UGC-NET Junior research fellowship and Commonwealth Scholarship Commission in the UK through Commonwealth Split-site PhD scholarship.

Competing Interests

The authors have no relevant financial or non-financial interests to disclose.

Author Contributions

JLW, JT, MSS and ALR were involved in planning and supervised the work, MSS carried out the experiment on the field. MSS and CY performed the analysis in the laboratory. MSS drafted the manuscript, designed the figures and performed the numerical calculations with inputs from JLW, JT and ALR. JLW, JT, ALR, CY and NJR provided critical feedback and helped shape the research, analysis and manuscript. All authors read and approved the final manuscript.

Data Availability

The data that support the findings of this study are available from the corresponding author, upon request.